Journal Name

ARTICLE TYPE

Cite this: DOI: 00.0000/xxxxxxxxxx

Linear Scaling Relationships in Homogeneous Photoredox Catalysis†

Kareesa J Kron,[a] and Shaama Mallikarjun Sharada[a,b]*

Received Date
Accepted Date

DOI: 00.0000/xxxxxxxxxx

This work investigates two competing pathways for the terphenyl radical anion in the photoredox catalytic cycle for CO_2 reduction – the desired electron transfer to CO_2 and the undesired carboxylation and deactivation of the terphenyl catalyst. A linear relationship is identified between the energetics of the two pathways when trends are examined via p-substitutions to the three isomeric forms of terphenyl. Analogous to linear scaling relationships in heterogeneous and electrocatalysis, this correlation highlights intrinsic bounds for catalyst performance towards photoredox CO_2 reduction.

Computational studies of heterogeneous catalytic processes, in which reactions occur at a solid-fluid interface, are typically guided by the fact that the interactions of various reactive intermediates with the catalyst surface are not independent of each other. Also termed scaling relationships for mapping activity or selectivity, the energies of interaction of specific intermediates and/or transition states are typically linearly correlated across catalysts.[1] In addition to reducing the complexity associated with catalyst design to a handful of descriptors, scaling relationships highlight fundamental limitations imposed by the underlying chemistry that makes it difficult to 'break' or circumvent them in order to enhance catalyst performance.[2]

Efforts towards developing similar design rules are now emerging in molecular thermal catalysis,[3–6] but almost non-existent in molecular photoredox chemistry. Photoredox catalysis is rapidly emerging as a sustainable alternative to traditional thermal catalysis as it can use light energy to perform otherwise challenging oxidation and reduction reactions.[7–10] Our objective is to uncover similar relationships that may exist in homogeneous photoredox catalytic processes, specifically those involving organic catalysts (chromophores) for carrying out the reduction of CO_2.[11–13] The photoredox catalytic cycle consists of electronic excitation of the catalyst, quenching of the excited state by means of a sacrificial electron donor (e.g., triethylamine) to create a highly reactive radical anion, and subsequent single-electron reduction of CO_2 by the radical anion, restoring the catalyst to its neutral, ground state. An experimental study probing the CO_2 reduction activity of terphenyls showed that the *ortho-* and *meta-* isomers are more prone to carboxylation (Figure 1) than the *para-* isomer, making the latter a more suitable catalyst for carrying out CO_2 reduction via electron transfer despite its smaller driving force relative to the other two isomers.[14] The competing carboxylation reaction is one possible reason why catalyst turnover numbers are very low. While designing these catalysts, therefore, it is not only important to identify features that render the catalyst more active but also those that make it less susceptible to degradation.[15,16]

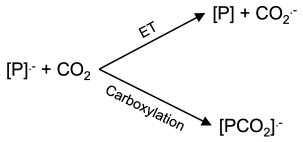

Fig. 1 Fate of the photoredox catalyst (P) in its radical anion state (1) Desired – Electron transfer (ET) to CO_2, or (2) Undesired – Carboxylation. Note that the possibility of interconversion between the ET and carboxylation state[17] is not considered in this work.

All simulations are carried out using the ab initio quantum chemistry software, Q-Chem.[18] We employ the ωB97X-D/def2-TZVP[19,20] level of theory along with the conductor-like polarizable continuum model[21–23] to capture the impact of solvation by dichlormethane (CH_2Cl_2, $\varepsilon = 8.93$). The reactant state for both ET and carboxylation consists of the catalyst anion and neutral CO_2, both at infinite separation. The sum of energies of the two fragment is labeled E_{react}. This is analogous to the 'isolated gas phase' reference typically employed in heterogeneous catalysis calculations of adsorption energies. The energy of the ET product ($E_{prod,ET}$) is calculated using constrained DFT (CDFT)[24–26]

[a] *Mork Family Department of Chemical Engineering and Materials Science, University of Southern California, Los Angeles CA, USA.*
[b] *Department of Chemistry, University of Southern California, Los Angeles CA, USA.*
*-*E-mail: ssharada@usc.edu*

† Electronic Supplementary Information (ESI) available. See DOI: 00.0000/00000000.

for the interacting fragments; analogous to adsorbed species in heterogeneous catalysis. The electronic energy change associated with electron transfer is given by

$$\Delta E_{ET} = E_{prod,ET} - E_{react} \quad (1)$$

The energies of carboxylation products ($E_{prod,carboxy}$) formed via electrophilic attack of every unique carbon position are calculated. Since position-dependent barrier calculations are computationally intensive, we make a simplifying assumption that the reaction energy is an approximate proxy for barriers. We define the reaction energy for carboxylation as

$$\Delta E_{carboxy} = E^{min}_{prod,carboxy} - E_{react} \quad (2)$$

In other words, the position that yields the lowest value of reaction energy is also assumed to correspond to the smallest barrier to carboxylation and therefore the most likely point of electrophilic attack. The *o*-, *m*-, and *p*- isomers of terphenyl, with two substituents each at the terminal *para*-positions, as shown in Figure 2, are examined. The following substituents are chosen: H, CH_3, OCH_3, CHO, CF_3, OH, F, NH_2, SCH_3, and NO_2.

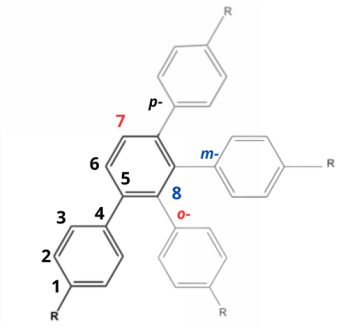

Fig. 2 Photoredox catalysts examined in this study - three isomeric forms of terphenyl with substituents R at the *para*-terminal positions. The carbon numbers indicate unique positions at which carboxylation can occur for every isomer.

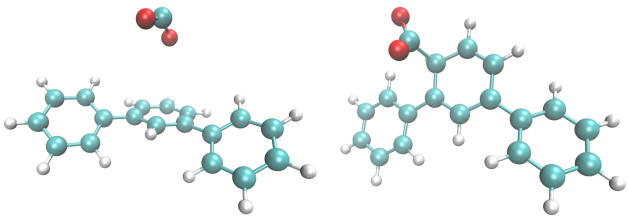

Fig. 3 Products of (left) ET and (right) carboxylation at position 6, illustrated for *m*-terphenyl. The shortest C-C distance between the radical anion CO_2 and a ring carbon is 4.596 Å in the ET product. The C-C distance in the carboxyl bond is 1.593 Å. (Cyan: Carbon; white: Hydrogen, red: Oxygen)

The structures associated with ET and carboxylation products are shown in Figure 3. The driving forces associated with competing ET and carboxylation are showed in Table 1. The higher ΔE_{ET} for the *p*- isomer arises from the fact that the radical anion form (or the reactant) is lower in energy for this isomer. The products formed upon ET for the three isomeric forms are within 8 kJ/mol of each other for each substitution. The sole exception is the NO_2-bound systems for which the *m*- and *o*- forms of the radical anion are significantly more stable than *p*-. In general, $\Delta E_{carboxy}$ is more negative than ΔE_{ET}. $\Delta E_{carboxy}$ values are more positive for the *p*- isomer arise, in addition to lower reactant energies, from differences in the preferred position and consequently energy of the carboxylation product.

Table 1 The driving forces for electron transfer and carboxylation (kJ/mol) for substituted *p*-, *m*-, and *o*-terphenyl calculated using DFT.

Group	σ_p	ΔE_{ET} (kJ/mol)			$\Delta E_{carboxy}$ (kJ/mol)		
		p-	*m*-	*o*-	*p*-	*m*-	*o*-
NH_2	-0.66	-43.6	-57.1	-66.6	-65.8	-79.4	-80.7
OH	-0.37	-35.2	-49.6	-58.0	-73.7	-71.9	-70.6
OCH_3	-0.27	-39.4	-51.5	-61.2	-55.0	-72.8	-78.2
CH_3	-0.17	-21.9	-38.5	-47.1	-36.9	-60.7	-56.1
H	0.00	-12.6	-29.2	-38.1	-27.3	-52.4	-46.6
SCH_3	0.00	-3.5	-11.2	-29.1	-22.6	-41.1	-46.1
F	0.06	-16.9	-32.8	-40.7	-33.9	-55.9	-54.0
CF_3	0.54	21.4	5.4	-3.1	-0.9	-22.7	-16.7
CHO[a]	0.63	63.9	60.8	54.7	33.1	28.5	23.2
NO_2[a]	1.27	85.6	127.3	125.4	46.7	87.4	85.3

[a] σ^* used instead of σ_P for CHO and NO_2.[27]

The preferred positions of carboxylation across the three isomers are illustrated in Figure 4. Carbon atoms on the terminal ring (1-3 in Figure 2) are favored for both *o*- and *p*-substituted isomers, while position 6 in the central ring is favored for *me*-isomers. The differences in $\Delta E_{carboxy}$ values between the position that is preferred the most across substituents (2 for *o*-, 6 for *m*-, and 2 for *p*-) and the next preferred positions are typically < 10 kJ/mol, with the sole exception of *p*-terphenyl, in which the difference between positions 3 and 2 is 12.5 kJ/mol. While some positions are clearly more favorable than others, it may be difficult to generalize these results to predict *a priori* the most favorable position for carboxylation for a given isomeric/substituted chromophore. The search for descriptors that help identify the preferred position of electrophilic attack is ongoing in our group.

As predicted by experiments and shown in our prior study, the reaction energy for carboxylation is more negative for the *o*- and *m*- isomers compared to the *p*-isomer of H-substituted terphenyl (Table 1).[14,16] Using the values for H-substituted *p*-terphenyl as reference, trends with changing substituent electrophilicity, quantified by the Hammett parameter, σ_p,[28] are reported in Figure 5. Since three distinct curves can be plotted, one for each isomeric form, we attempt to identify an alternative descriptor to the Hammett parameter that eliminates isomer specificity. Mulliken charges on the catalyst (excluding substituent), shown in Figure S1 of the ESI, are poor descriptors of energetics of electron transfer and carboxylation. The resulting correlations are significantly weaker than those observed with Hammett parameters.

As seen in Figure 5, with the exception of the NO_2-substituted systems, the *o*- and *m*- isomeric forms of substituted systems are also more susceptible to carboxylation than the *p*-isomer. Electron-donating groups render both competing pathways more energetically favorable. The trends are non-linear, with a flattening of the driving force as substituents become more electron-

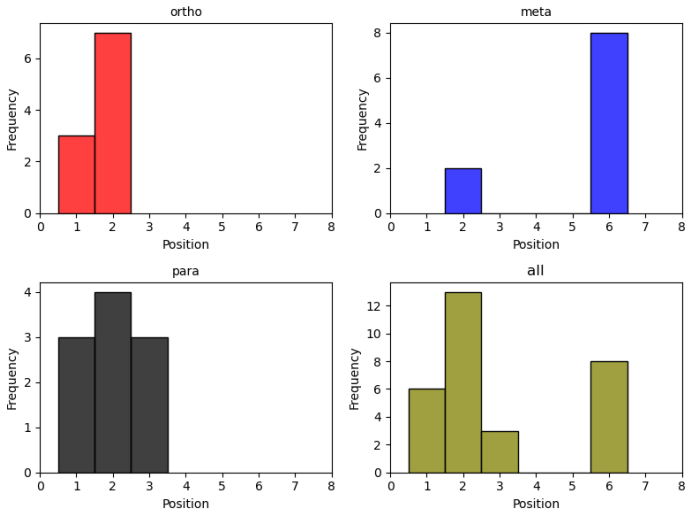

Fig. 4 Carbon positions (Figure 2) with the lowest $\Delta E_{carboxy}$ across all substituted terphenyls.

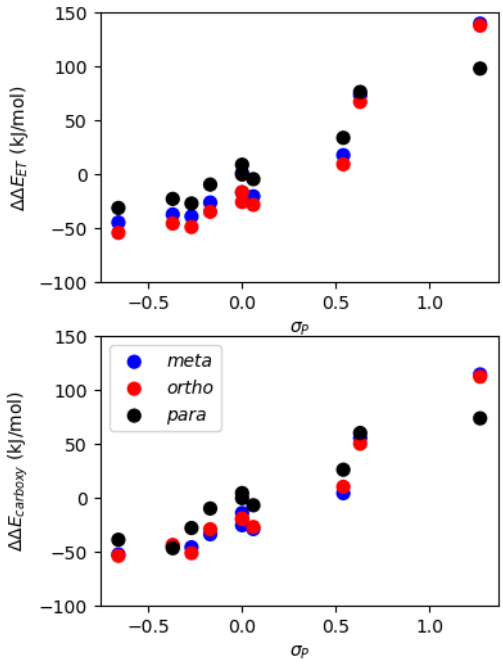

Fig. 5 Variation in ET and carboxylation energies, referenced to the corresponding values obtained for the H-substituted *para*-terphenyl, with the Hammett electrophlicity parameter.

donating. This was also observed in our previous work examining the ET activity of substituted *p*-terphenyl towards CO_2 reduction.[15]

The anomalous energetics of NO_2-substituted systems is examined using localized orbital bonding analysis (LOBA).[29] The orbital densities associated with the excess electron in the anion radical form of the chromophore are illustrated in Figure S2 of the ESI. Unlike the remaining substituted *o*- and *m*- isomers in which the electron is delocalized over two to four ring carbon atoms, density is localized about the nitrogen of the NO_2 and one neighboring carbon atom. This localization is not observed in the NO_2-substituted *p*-terphenyl, in which the electron is delocalized over four ring carbons. We believe that this anomalous localization at the strongly electron-withdrawing substituent may be the cause of lower energies of the *m*- and *o*- radical anions relative to the *p*- radical anion.

As the ET and carboxylation trends with respect to σ_p in Figure 5 look very similar to each other, we examine whether the two quantities are correlated. Shown in Figure 6, a linear relationship emerges spanning all isomeric forms and all substitutions to terphenyl. This finding is probably not surprising. Electron-donating substituents make it easier to transfer an excess electron to an electrophile such as CO_2. At the same time if the two species are in close proximity, it is likely that bond formation also becomes favorable. Figure 6 therefore indicates that one cannot enhance the driving force for ET (desirable) without also making the catalyst more susceptible to degradation via carboxylation or similar electrophilic reactions such as photo-Birch reduction.[30] In other words, a scaling relationship exists between the energetics of ET and carboxylation pathways, which originates in the electronic properties of the catalyst.

In computational heterogeneous catalysis and electrocatalysis, linear scaling relationships can be identified between adsorption or transition state energies of different, but related species adsorbed on the surfaces of transition metals (e.g., C* and COH* or CO* and COOH* in CO_2 reduction, where * denotes a surface-adsorbed species and not an excited state).[31,32] Once these limitations are identified, one can then explore options for circumventing them, such as alloying, doping, and the introduction of defects or strain in the solid catalyst.[2,33]

The concept of 'breaking' these scaling relationships can also be applied to organic photoredox catalysis. In this study, although $\Delta E_{carboxy}$ is more negative than ΔE_{ET} for a given system, the energy alone is not a complete descriptor of the likelihood of reaction when one of the competing pathways involves electron transfer. Unlike bond formation, ET can occur (1) at large intermolecular separations, (2) when steric bulk prevents close contact between donor-acceptor pairs, and (3) with less specificity in the orientation necessary for the reaction to occur, and therefore possesses an entropic advantage.[34,35] The solvent dielectric may also play a role in the relative rates of the two pathways. Carboxylation becomes less favorable in a solvent of higher dielectric as charge is more delocalized in both the transition state and product, as a result of which they are more difficult to solvate.[36]

Therefore, it may be possible to break scaling by introducing steric constraints and identifying solvents that are less favorable towards the approach of the anion radical catalyst and CO_2 and subsequent formation of a pre-association complex that leads to carboxylation. This work is a simple first step that focuses only one part of the entire photoredox catalytic cycle for CO_2 reduction to explore the existence of scaling relationships. Future work in our group, in addition to examining whether the assumption that the lowest reaction energy also corresponds to the smallest barrier to carboxylation is valid, will include an examination of whether substitutions at positions other than *p*- lead to energies that lie on

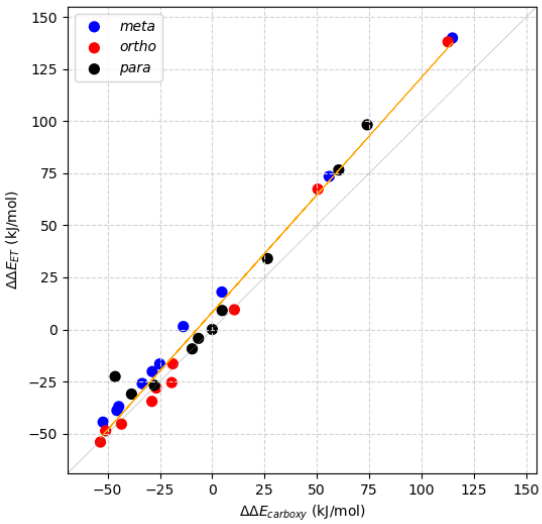

Fig. 6 Scaling relationship between ET and carboxylation energies, referenced to the corresponding values obtained for H-substituted *para*-terphenyl. The orange line represents the linear fit ($R^2 = 0.99$), with $\Delta\Delta E_{ET} = 1.13\ \Delta\Delta E_{carboxy} + 8.22$. The parity line is also shown (light grey).

the same scaling line and if solvent effects can be incorporated in a meaningful manner in catalyst design.

This material is based upon work supported by the National Science Foundation under Grant No. 2102044. The authors are grateful to the Collaboratory for Advanced Research Computing at USC for computational resources and support.

Author Contributions

KJK and SMS carried out the computational work and analysis described in this study. SMS led the design of simulations, fundraising, and manuscript writing.

Conflicts of interest

There are no conflicts to declare.

Notes and references

1 F. Abild-Pedersen, J. Greeley, F. Studt, J. Rossmeisl, T. R. Munter, P. G. Moses, E. Skulason, T. Bligaard and J. K. Nørskov, *Physical Review Letters*, 2007, **99**, 016105.
2 A. Vojvodic and J. K. Nørskov, *National Science Review*, 2015, **2**, 140–143.
3 T. Z. Gani and H. J. Kulik, *ACS Catalysis*, 2018, **8**, 975–986.
4 M. Anand and J. K. Nørskov, *ACS Catalysis*, 2019, **10**, 336–345.
5 P. C. Andrikopoulos, C. Michel, S. Chouzier and P. Sautet, *ACS Catalysis*, 2015, **5**, 2490–2499.
6 Z. Lan and S. Mallikarjun Sharada, *Physical Chemistry Chemical Physics*, 2021, **23**, 15543–15556.
7 N. A. Romero and D. A. Nicewicz, *Chemical Reviews*, 2016, **116**, 10075–10166.
8 M. H. Shaw, J. Twilton and D. W. MacMillan, *The Journal of Organic Chemistry*, 2016, **81**, 6898–6926.
9 M. Majek and A. Jacobi Von Wangelin, *Accounts of Chemical Research*, 2016, **49**, 2316–2327.
10 C. Stephenson and T. Yoon, *Accounts of Chemical Research*, 2016, **49**, 2059–2060.
11 S. Matsuoka, T. Kohzuki, C. Pac and S. Yanagida, *Chemical Letters*, 1990, **19**, 2047–2048.
12 C. R. Jamison and L. E. Overman, *Accounts of Chemical Research*, 2016, **49**, 1578–1586.
13 H. Seo, M. H. Katcher and T. F. Jamison, *Nature Chemistry*, 2017, **9**, 453.
14 S. Matsuoka, T. Kohzuki, C. Pac, A. Ishida, S. Takamuku, M. Kusaba, N. Nakashima and S. Yanagida, *The Journal of Physical Chemistry*, 1992, **96**, 4437–4442.
15 K. J. Kron, S. J. Gomez, Y. Mao, R. J. Cave and S. Mallikarjun Sharada, *Journal of Physical Chemistry A*, 2020, **124**, 5359–5368.
16 K. J. Kron, A. Rodriguez-Katakura, P. Regu, M. N. Reed, R. Elhessen and S. Mallikarjun Sharada, *The Journal of Chemical Physics*, 2022, **156**, year.
17 J. M. Saveant, *Accounts of Chemical Research*, 1993, **26**, 455–461.
18 E. Epifanovsky, A. T. B. Gilbert, X. Feng, J. Lee, Y. Mao, N. Mardirossian, P. Pokhilko, A. F. White, M. P. Coons, A. L. Dempwolff, Z. Gan, D. Hait, P. R. Horn, L. D. Jacobson, I. Kaliman, J. Kussmann, A. W. Lange, K. U. Lao, D. S. Levine, J. Liu, S. C. McKenzie, A. F. Morrison, K. D. Nanda, F. Plasser, D. R. Rehn, M. L. Vidal, Z.-Q. You, Y. Zhu, B. Alam, B. J. Albrecht, A. Aldossary, E. Alguire, J. H. Andersen, V. Athavale, D. Barton, K. Begam, A. Behn, N. Bellonzi, Y. A. Bernard, E. J. Berquist, H. G. A. Burton, A. Carreras, K. Carter-Fenk, R. Chakraborty, A. D. Chien, K. D. Closser, V. Cofer-Shabica, S. Dasgupta, M. de Wergifosse, J. Deng, M. Diedenhofen, H. Do, S. Ehlert, P.-T. Fang, S. Fatehi, Q. Feng, T. Friedhoff, J. Gayvert, Q. Ge, G. Gidofalvi, M. Goldey, J. Gomes, C. E. Gonzalez-Espinoza, S. Gulania, A. O. Gunina, M. W. D. Hanson-Heine, P. H. P. Harbach, A. Hauser, M. F. Herbst, M. Hernandez Vera, M. Hodecker, Z. C. Holden, S. Houck, X. Huang, K. Hui, B. C. Huynh, M. Ivanov, A. Jasz, H. Ji, H. Jiang, B. Kaduk, S. Kahler, K. Khistyaev, J. Kim, G. Kis, P. Klunzinger, Z. Koczor-Benda, J. H. Koh, D. Kosenkov, L. Koulias, T. Kowalczyk, C. M. Krauter, K. Kue, A. Kunitsa, T. Kus, I. Ladjanszki, A. Landau, K. V. Lawler, D. Lefrancois, S. Lehtola, R. R. Li, Y.-P. Li, J. Liang, M. Liebenthal, H.-H. Lin, Y.-S. Lin, F. Liu, K.-Y. Liu, M. Loipersberger, A. Luenser, A. Manjanath, P. Manohar, E. Mansoor, S. F. Manzer, S.-P. Mao, A. V. Marenich, T. Markovich, S. Mason, S. A. Maurer, P. F. McLaughlin, M. F. S. J. Menger, J.-M. Mewes, S. A. Mewes, P. Morgante, J. W. Mullinax, K. J. Oosterbaan, G. Paran, A. C. Paul, S. K. Paul, F. Pavosevic, Z. Pei, S. Prager, E. I. Proynov, A. Rak, E. Ramos-Cordoba, B. Rana, A. E. Rask, A. Rettig, R. M. Richard, F. Rob, E. Rossomme, T. Scheele, M. Scheurer, M. Schneider, N. Sergueev, S. Mallikarjun Sharada, W. Skomorowski, D. W. Small, C. J. Stein, Y.-C. Su, E. J. Sundstrom, Z. Tao, J. Thirman, G. J. Tornai, T. Tsuchimochi, N. M. Tubman, S. P. Veccham, O. Vydrov, J. Wenzel, J. Witte, A. Yamada, K. Yao, S. Yeganeh, S. R. Yost, A. Zech, I. Y. Zhang, X. Zhang, Y. Zhang, D. Zuev, A. Aspuru-Guzik, A. T. Bell, N. A. Besley, K. B. Bravaya, B. R. Brooks, D. Casanova, J.-D. Chai, S. Coriani, C. J. Cramer, G. Cserey, A. E. DePrince, R. A. DiStasio, A. Dreuw, B. D. Dunietz, T. R. Furlani, W. A. Goddard, S. Hammes-Schiffer, T. Head-Gordon, W. J. Hehre, C.-P. Hsu, T.-C. Jagau, Y. Jung, A. Klamt, J. Kong, D. S. Lambrecht, W. Liang, N. J. Mayhall, C. W. McCurdy, J. B. Neaton, C. Ochsenfeld, J. A. Parkhill, R. Peverati, V. A. Rassolov, Y. Shao, L. V. Slipchenko, T. Stauch, R. P. Steele, J. E. Subotnik, A. J. W. Thom, A. Tkatchenko, D. G. Truhlar, T. Van Voorhis, T. A. Wesolowski, K. B. Whaley, H. L. Woodcock, P. M. Zimmerman, S. Faraji, P. M. W. Gill, M. Head-Gordon, J. M. Herbert and A. I. Krylov, *The Journal of Chemical Physics*, 2021, **155**, 084801.
19 J.-D. Chai and M. Head-Gordon, *Physical Chemistry Chemical Physics*, 2008, **10**, 6615–6620.
20 J.-D. Chai and M. Head-Gordon, *The Journal of Chemical Physics*, 2008, **128**, 084106.
21 T. N. Truong and E. V. Stefanovich, *Chemical Physics Letters*, 1995, **240**, 253 – 260.
22 V. Barone and M. Cossi, *The Journal of Physical Chemistry A*, 1998, **102**, 1995–2001.
23 M. Cossi, N. Rega, G. Scalmani and V. Barone, *Journal of Computational Chemistry*, 2003, **24**, 669–681.
24 Q. Wu and T. Van Voorhis, *Journal of Chemical Theory and Computation*, 2006, **2**, 765–774.
25 Q. Wu and T. Van Voorhis, *The Journal of Physical Chemistry A*, 2006, **110**, 9212–9218.
26 Q. Wu and T. Van Voorhis, *The Journal of Chemical Physics*, 2006, **125**, 164105.
27 H. H. Jaffé, *Chemical Reviews*, 1953, **53**, 191–261.
28 L. P. Hammett, *Journal of the American Chemical Society*, 1937, **59**, 96–103.
29 A. J. Thom, E. J. Sundstrom and M. Head-Gordon, *Physical Chemistry Chemical Physics*, 2009, **11**, 11297–11304.
30 J. A. Barltrop, *Pure and Applied Chemistry*, 1973, **33**, 179–196.
31 M. J. Kolb, D. Loffreda, P. Sautet and F. Calle-Vallejo, *Journal of Catalysis*, 2021, **395**, 136–142.
32 A. A. Peterson and J. K. Nørskov, *The Journal of Physical Chemistry Letters*, 2012, **3**, 251–258.
33 J. Pérez-Ramírez and N. López, *Nature Catalysis*, 2019, **2**, 971–976.
34 J. M. Saveant, *Journal of the American Chemical Society*, 1992, **114**, 10595–10602.
35 A. Pross, *Accounts of Chemical Research*, 1985, **18**, 212–219.
36 R. Marcus, *The Journal of Physical Chemistry A*, 1997, **101**, 4072–4087.